Hadron and linear collider probes of hidden-sector gauge bosons

Jason Kumar[1] and James D. Wells[2]

[1]*Physics Department, Texas A&M University, College Station, Texas 77843, USA*
[2]*Michigan Center for Theoretical Physics (MCTP) Department of Physics, University of Michigan, Ann Arbor, Michigan 48109, USA*

Intersecting D-brane theories motivate the existence of exotic $U(1)$ gauge bosons that only interact with the standard model through kinetic mixing with hypercharge. We analyze an effective field theory description of this effect and describe the implications of these exotic gauge bosons on precision electroweak, LHC, and ILC observables.

I. EXOTIC ABELIAN SYMMETRIES

There are many reasons to suspect that nature contains more Abelian factors than just hypercharge of the standard model (SM). Traditionally, these Abelian groups were thought to arise as subgroups of larger unification groups, such as $SO(10) \rightarrow G_{SM} \times U(1)$ or $E_6 \rightarrow G_{SM} \times U(1)^2$ [1]. This motivation for extra $U(1)$ gauge groups led to studies of exotic Z' bosons that coupled at tree level to the SM particles [2–4].

In this paper, we wish to emphasize the intersecting braneworld motivation for extra $U(1)$ factors and study their consequences for phenomenology within an effective theory framework. In these constructions, one considers string theory compactified to four dimensions with spacetime-filling D-branes wrapping cycles in the compact dimensions. The open strings which begin and end on the D-branes yield a low-energy gauge theory which can potentially realize the standard model. Although there are not yet any known intersecting brane models that have been completely worked out and are free of phenomenological problems, this class of string constructions is very broad, with a staggering number of potentially viable vacua [5,6]. As such, it seems reasonable to assume that there are models in this general class that can closely approximate observed low-energy physics, and a study of phenomenology generic to this class becomes quite interesting.

To begin with, we note a basic fact: a stack of N coincident branes gives rise to the gauge group $U(N)$, which is decomposed into $SU(N) \times U(1)$. There are typically many stacks of coincident branes in a complete, self-consistent string theory of particle physics. Unless the branes are at special points in the extra-dimensional space, they will produce at least one Abelian factor for every stack. Of these, a few combinations are anomaly free and massless (see, e.g., Refs. [7–12]).

Braneworld $U(1)$'s are special (compared to GUT $U(1)$'s) because there is no generic expectation that SM particles will be charged under them. When a SM-like theory is constructed in braneworld scenarios, the SM particles generally arise as open strings connecting one SM brane stack to another. Exotic non-SM branes usually carry the extra $U(1)$ factors. However, there are exotic states, called kinetic messengers below, that can be charged under the SM gauge group and the exotic $U(1)$. These arise from open strings connecting a SM brane stack to a hidden-sector brane stack. These states can generate kinetic mixing between the $U(1)_Y$ and an exotic $U(1)$ symmetry that has phenomenological implications to be explored below.

Despite our D-brane motivations given above, we wish to transition to an effective field theory description for our discussion of phenomenological implications. This, we believe, is a useful approach to string phenomenology: identify a generic aspect of string theory (e.g., hidden-sector $U(1)$'s described above), embed the specific idea into a more general effective field theory framework, and then explore the phenomenological implications of the wider range of parameters in the effective theory.

In the next section we set out the effective theory description. We then describe several of the phenomenological implications of this straightforward but interesting generic implication of D-brane scenarios. The implications surveyed are those of precision electroweak constaints, Large Hadron Collider (LHC) detection prospects, and International Linear Collider (ILC) detection prospects.

II. EFFECTIVE THEORY DESCRIPTION

The framework described above gives rise to the possibility that an exotic $U(1)_X$ gauge symmetry exists that survives down to the TeV scale, but has no direct couplings to SM particles. Our effective field theory description at a scale $\Lambda \gg m_Z$ has standard model (SM) gauge group and an additional $U(1)_X$. There are three sectors of matter particles

(i) *Visible sector:* Particles charged under the SM but not under $U(1)_X$. The SM particles (quarks, leptons, Higgs, neutrinos) comprise this sector.

(ii) *Hidden sector:* Particles charged under $U(1)_X$, but singlets under the SM gauge groups.

(iii) *Hybrid sector:* Particles charged under both the SM and $U(1)_X$ gauge groups, which we call *kinetic messengers* since they can induce kinetic mixing between $U(1)_X$ and SM hypercharge.

For our purposes, we will assume that $U(1)_X$ is broken by a Higgs mechanism. The mass-scale associated with X

breaking can be assumed for this discussion to be tied to the same mass scale that gives rise to electroweak symmetry breaking. For example, softly broken supersymmetry masses could provide the requisite Higgs masses for various sectors that all break the respective gauge symmetries around the same supersymmetry breaking gravitino mass.

There are one-loop quantum corrections that mix the kinetic terms of $U(1)_Y$ and $U(1)_X$ [13–19]. We are then left with an effective Lagrangian at scale μ for the kinetic terms of the form:

$$L_K = -\frac{1}{4}\hat{B}_{\mu\nu}\hat{B}^{\mu\nu} - \frac{1}{4}\hat{X}_{\mu\nu}\hat{X}^{\mu\nu} + \frac{\chi}{2}\hat{B}_{\mu\nu}\hat{X}^{\mu\nu}, \quad (1)$$

where χ is given by

$$\chi = \frac{\hat{g}_Y\hat{g}_X}{16\pi^2}\sum_i Q_X^i Q_Y^i \log\left(\frac{m_i^2}{\mu^2}\right), \quad (2)$$

and the sum i is over all kinetic messenger states.

We cannot say what value of χ is typical in the many possible braneworld models of particle physics [20]. Although the above equation is a one-loop expression, and perhaps expected to be small, the multiplicity of states could be large enough to compensate for the one-loop suppression. In a different context, the issue of kinetic mixing among exotic $U(1)$'s was investigated by Dienes, Kolda, and March-Russell [13], and it was estimated that $10^{-3} < \chi < 10^{-2}$; however, this estimate may not be applicable for other approaches to model building.

One can choose a field redefinition $\hat{X}_\mu$, $\hat{Y}_\mu \to X_\mu$, Y_μ that makes the kinetic terms of Eq. (1) diagonal and canonical. The most convenient choice of diagonalization is one in which the couplings to Y are independent of Q_X:

$$\begin{pmatrix} X_\mu \\ Y_\mu \end{pmatrix} = \begin{pmatrix} \sqrt{1-\chi^2} & 0 \\ -\chi & 1 \end{pmatrix}\begin{pmatrix} \hat{X}_\mu \\ \hat{Y}_\mu \end{pmatrix}. \quad (3)$$

The covariant derivative is now

$$D_\mu \to \partial_\mu + i(g_X Q_X + \eta g_Y Q_Y)X_\mu + ig_Y Q_Y Y_\mu, \quad (4)$$

where

$$g_Y = \hat{g}_Y, \qquad g_X \equiv \frac{\hat{g}_X}{\sqrt{1-\chi^2}}, \qquad \eta \equiv \frac{\chi}{\sqrt{1-\chi^2}}. \quad (5)$$

(Note, $\eta \simeq \chi$ for small χ.) We are considering the case where $U(1)_X$ is broken due to the veving of a hidden-sector Higgs field Φ_X with $Q_X \neq 0$ and $Q_Y = 0$. X_μ then gets a mass $m_X^2 \sim g_X^2\langle\Phi_X\rangle^2$, while Y stays massless. It is somewhat natural that m_X is of order weak scale or TeV scale, especially if the vev is controlled by supersymmetry breaking, as suggested earlier. Note, the covariant derivative couples matter to Y in the same way as to $\hat{Y}$. Thus, we can identify Y as the hypercharge gauge boson.

SM particles couple to X^μ with strength $\eta g_Y Q_Y$, i.e. with couplings proportional to hypercharge. This is an important phenomenological implication that enables X_μ

to be probed by experiments involving SM particles. The X_μ behaves as a resonance of the hypercharge gauge boson with somewhat smaller coupling; indeed, it may be confused with an extra-dimension hypercharge gauge boson. It is also within the general class of ''Y-sequential'' gauge boson [21].

The $U(1)_X$ also couples to hidden-sector fields at tree level. However, we assume the $U(1)_X$ gauge boson we are studying is too light to decay into on-shell hidden-sector particles or exotic kinetic messengers. Intersecting brane models generally have multiple hidden-sector gauge group factors, which can break at different scales. But light matter will appear in chiral multiplets arising from strings stretching between different branes, and their mass will be set by the hidden-sector gauge-symmetry breaking scales of the two gauge groups under which matter is charged. If we study the hidden $U(1)_X$ which is broken at the lowest scale, the mass of most hidden-sector matter will be dominated by the higher symmetry breaking scales of other gauge groups, and our assumption about the lightness of the $U(1)_X$ gauge boson relative to other hidden matter is likely correct. If this assumption is wrong, the collider signatures that rely on branching fractions of X boson decays into SM particles would have to be adjusted. Given the small kinetic mixing angle we envision, if the X does decay into long-lived hidden-sector states it is likely that the ILC searches described below for γX production, where γ recoils against ''nothing'' would be most useful. Analogous LHC monojet or monophoton signals would need to be studied in that case as well. If the X decays into long-lived charged, exotic messenger states, the quasistable massive charged particle search strategies would be useful.

III. MASS EIGENSTATES AFTER ELECTROWEAK SYMMETRY BREAKING

When $SU(2) \times U(1)_Y$ breaks to $U(1)_{\text{em}}$, the Z_μ and X_μ eigenvalues mix due to the small coupling of X_μ to condensing Higgs boson(s) that carry hypercharge. The effects of this mixing are minimal for the phenomenology of the X_μ boson at high-energy colliders, except for two effects. First, the mixing with the Z boson gives contributions to precision electroweak observables. Computing observables from effective Peskin-Takeuchi parameters [19,22,23], one finds the shifts

$$\Delta m_W = (17 \text{ MeV})\Upsilon, \quad (6)$$

$$\Delta\Gamma_{l^+l^-} = -(8 \text{ keV})\Upsilon, \quad (7)$$

$$\Delta\sin^2\theta_W^{\text{eff}} = -(0.00033)\Upsilon, \quad (8)$$

where

$$\Upsilon \equiv \left(\frac{\eta}{0.1}\right)^2\left(\frac{250 \text{ GeV}}{m_X}\right)^2. \quad (9)$$

Experimental measurements [24] of these most important electroweak observables put limits on $|Y| \lesssim 1$. Thus, for kinetic mixing of $\eta \lesssim \mathcal{O}(0.1)$ current precision electroweak observables do not constrain our effective theory as long as m_X is greater than several hundred GeV. No meaningful bound for any value of η results if m_X is greater than about a TeV. This fact is consistent with the precision electroweak analysis of all other weakly coupled Z' bosons that are summarized nicely in the particle data group listings [25].

The second consequence is that the mixing between the Z and X bosons can change the hypercharge coupling of X to SM particles. This is a subdominant effect for small m_Z^2/m_X^2, except it now allows the X mass eigenstate to decay into SM bosons. After mixing, and assuming large m_X, one finds

$$\Gamma(WW) \simeq \Gamma(Zh) \simeq \eta^2 (0.21 \text{ GeV})\left(\frac{m_X}{1 \text{ TeV}}\right), \quad (10)$$

each of which is less than 2% of the total width to fermions, calculated from summing all

$$\Gamma(f\bar{f}) \simeq N_c \eta^2 (1.7 \text{ GeV})(Y_{f_L}^2 + Y_{f_R}^2)\left(\frac{m_X}{1 \text{ TeV}}\right). \quad (11)$$

Because the branching fraction is not large, we ignore bosonic decays in the subsequent analysis.

IV. LHC AND TEVATRON PROBES

We are now in a position to examine the possible collider signatures of this scenario. The process most amenable to LHC analysis is on-resonance $pp \to X \to \mu\bar{\mu}$. The predominant backgrounds are $pp \to \gamma^*/Z^* \to \mu\bar{\mu}$.

For a hadron collider, observational bounds are somewhat model-independent. If we denote by N_X the number of signal events needed for a discovery signal, we find that the limit on the mass of a discoverable X is [3,4]

$$m_X^{\lim} \simeq \frac{\sqrt{s}}{A} \ln\left(\frac{L}{s}\frac{c_X C}{N_X}\right), \quad (12)$$

where the details of the model are encoded in

$$c_X = \frac{4\pi^2}{3}\frac{\Gamma_X}{m_X}B(\mu\bar{\mu})\left[B(u\bar{u}) + \frac{1}{C_{ud}}B(d\bar{d})\right].$$

For a pp ($p\bar{p}$) collider, $A = 32(20)$, $C = 600(300)$, and in the kinematical region of interest at LHC $C_{ud} \sim 2$ and $\sqrt{s} = 14$ TeV. L is the integrated luminosity. If $m_X > m_X^{\lim}$, X_μ cannot be observed at the collider. The logarithmic dependence of the detection bound implies that this result is rather robust, somewhat insensitive to variations in detector efficiency, number of events needed for discovery, or small variations in luminosity.

Substituting in the appropriate branching fractions $B(f\bar{f})$ yields $c_X(X \to \mu\bar{\mu}) = 0.00456\eta^2$ (for $m_X < 2m_{\text{top}}$, this will increase by $<15\%$). We will fix an inte-

grated luminosity of 100 fb^{-1}, which is expected from LHC after a few years of high-luminosity running. We then find

$$m_X^{\lim} \simeq 5.78 \text{ TeV} + (0.44 \text{ TeV})\ln\eta^2 - (0.44 \text{ TeV})\ln N_X$$

at 100 fb^{-1} integrated luminosity. Equivalently, we may write the lower limit on detectable kinetic mixing in terms of the mass of the X and the number of signal events N_X as

$$\eta \gtrsim \sqrt{N_X}e^{-6.61 + (m_X/0.88 \text{ TeV})}.$$

To turn the above expressions into estimated bounds on m_X, we need to determine how many signal events N_X are needed to discern the peak above background. Since for much of the parameter space, and, in particular, the parameter space near the edge of detectability for small η, the X boson is very narrow and we must take into account experimental resolution. The energy resolution of an invariant $\mu^+\mu^-$ peak is expected to be no better than a few percent [26]. Thus, we cannot choose bin sizes too small to maximize signal events over background events. For our parameter space, a minimum bin size of 50 GeV will become appropriate for any $m_X \lesssim 2$ TeV, which will be about the maximum value of m_X detectable if $\eta \lesssim 0.1$. The muon resolution decreases as m_X decreases, but the electron resolution gets better. Thus, we could substitute e^+e^- decay analysis for very massive m_X all the way up to $\eta \sim 1$ and $m_X \lesssim 5$ TeV, which is approximately the maximum value of m_X that one could hope for detecting a weakly coupled Z' boson at the LHC [27]. As we are interested in probing the smallest values of η it will not be necessary to consider that possibility further.

Using Pythia [28] to simulate the SM background in 50 GeV bins, we can then plot $\frac{N_X}{\sqrt{N_{\text{bgd}}}}$ at LHC as a function of η and m_X (Fig. 1). Detection at the LHC requires $N_X/\sqrt{N_{\text{bgd}}} > 5$ in a single bin normalized to a smooth SM background distribution. We see that realistic demands for a signal which can be distinguished from the back-
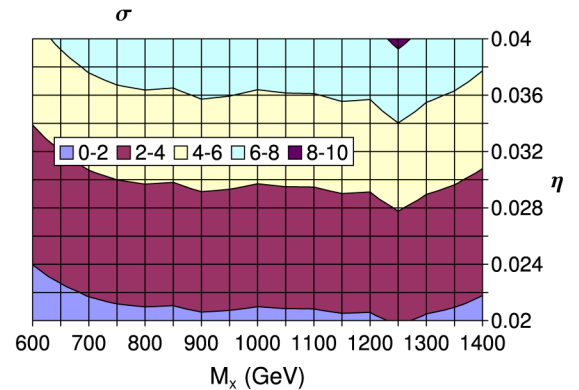

FIG. 1 (color online). LHC detection prospects for 100 fb^{-1} of integrated luminosity in the η-M_X plane. The contours are of signal significance, which exceeds 5 only when $\eta \gtrsim 0.03$.

ground will require $\eta > 0.03$. Below the top threshold, the bounds on η may shift by $<8\%$. Although this is unfortunately not a good probe when compared to naive one-loop perturbative estimates, the multiplicity of kinetic messengers may enable $\eta > 0.03$ and so should be studied with care at the LHC.

The analysis at Tevatron is similar, but with different parameters (accounting for differences in specifications and for a $p\bar{p}$ collider). We now have $C_{ud} = 25$ and $\sqrt{s} = 2$ TeV. Assuming an integrated luminosity of 8 fb^{-1}, the η sensitivity is

$$\eta_{\text{teva.}} \gtrsim \sqrt{N_X} e^{-6.7 + (m_X/0.2 \text{ TeV})}.$$

For detection we demand at least a 5σ signal above background, or at least 10 events above background (whichever is larger). At $m_X = 500$ GeV detection could only occur if $\eta > 0.07$ for this high luminosity. As m_X increases, the sensitivity limits on η degrade rapidly.

V. ILC PROSPECTS

Given the challenge for LHC detection posed by small kinetic mixing, one might hope that ILC can do better. An e^+e^- collider will generally trade away $\sqrt{s}$ for higher luminosity (~ 500 fb^{-1}) and a cleaner signal. One does not produce an X on resonance, of course, unless its mass is less than the center of mass energy, which we assume here to be 500 GeV.

The basic process we are interested in is $e^-e^+ \rightarrow \mu\bar{\mu}$ through $\gamma^*/Z^*/X^*$. The observable that provides perhaps the most useful signal in this case is the total cross section [29] (the forward-backward asymmetry and left-right polarization do not appear to provide qualitative improvement). We may write the total cross section as

$$\sigma_{\text{tot}}(f\bar{f}) = \frac{N_c}{48\pi s} \sum_{n,m} \frac{g_n^2 g_m^{*2} s^2 I_{m,n}^f}{(s - m_{V_n}^2)(s - m_{V_m}^2)^*}, \qquad (13)$$

where

$$I_{m,n}^f = (L_n^e L_m^{e*} + R_n^e R_m^{e*})(L_n^f L_m^{f*} + R_n^f R_m^{f*}), \qquad (14)$$

and the coupling of the V_n boson to the fermions $f\bar{f}$ is given by $ig_n\gamma^\mu(L_n^f P_L + R_n^f P_R)$. If $m_X > 500$ GeV, this observable will provide the dominant signal. Near the resonance, the signal is enhanced and we should replace

$$\frac{1}{s - m_V^2} \Rightarrow \frac{(s - m_V^2) - i\Gamma_V\sqrt{s}}{(s - m_V^2)^2 + s\Gamma_V^2} \Rightarrow \frac{-i}{\Gamma_V m_V}. \qquad (15)$$

Our strategy is to compare the inclusive cross section for X production to the pure standard model background. Our criterion for a signal detection is at least 1% deviation from SM expectations, in order not to run afoul of systematic uncertainties. Recall, we are assuming 500 fb^{-1} of integrated luminosity, and so the corresponding statistical significance of the signal is $\sim \mathcal{L}\sigma_S/\sqrt{\mathcal{L}\sigma_B} =$
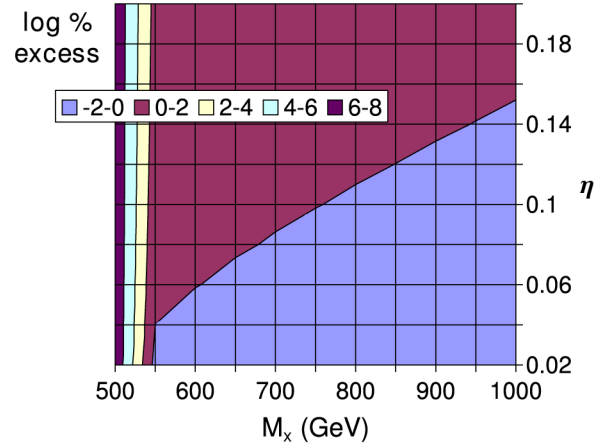

FIG. 2 (color online). Deviations of $e^+e^- \rightarrow \mu\bar{\mu}$ at ILC at $\sqrt{s} = 500$ GeV for 500 fb^{-1} integrated luminosity are represented in this plot as contours of the $\log_{10}(\%)$ of the excess of events produced compared to SM expectations. The line along the interface of the blue and maroon regions represents a $10^0 = 1\%$ (or $\sim 5\sigma$) deviation.

$0.01\sqrt{\mathcal{L}\sigma_B} \simeq 4.7 \sim 5\sigma$, given the SM cross section $\sigma_{\text{tot}} = 447$ fb [30]. Figure 2 shows the excess of $e^+e^- \rightarrow \mu\bar{\mu}$ events at ILC at $\sqrt{s} = 500$ GeV for 500 fb^{-1} integrated luminosity. Increasing values of M_X can be probed only by increasing values of the mixing parameter η. For example, $M_X = 750$ GeV (1000 GeV) can be probed for values of η as low as 0.10 (0.15).

If $m_X < 500$ GeV, then we should instead consider the hard-scattering process $e^-e^+ \rightarrow \gamma X \rightarrow \gamma f\bar{f}$. The emission of a hard photon will allow us to scatter through a resonance of the X, enhancing the cross section and yielding a cleaner signal. This is a leading order calculation, as radiation of more photons would serve to enhance both the signal and backgrounds we calculate for the single photon case.

The differential cross section of γX production is

$$\frac{d\sigma}{dx} = \frac{\alpha(c_L^2 + c_R^2)[(s + m_X^2)^2 + (s - m_X^2)^2 x^2]}{4s^2(s - m_X^2)(1 - x^2)}, \qquad (16)$$

where $x \equiv \cos\theta$ and $i\gamma^\mu(c_L P_L + c_R P_R)$ are the couplings of the left and right handed electrons to X_μ. We choose a standard $|\cos\theta| < 0.95$ angular cut. The signal we analyze[1] is $X \rightarrow \mu\bar{\mu}$, so we must multiply by the appropriate branching fraction, $B(\mu\bar{\mu}) = 0.12$. Substituting in the couplings we find

---

[1]We choose $\mu^+\mu^-$ as a specific final state, but detection of the X boson can come from any decay channel (including invisible) by looking for the peak in photon-recoil spectrum. Definitive final states, such as $\mu^+\mu^-$ invariant mass peak however are sharp signals of the X-boson mass and branching fraction into $\mu^+\mu^-$.
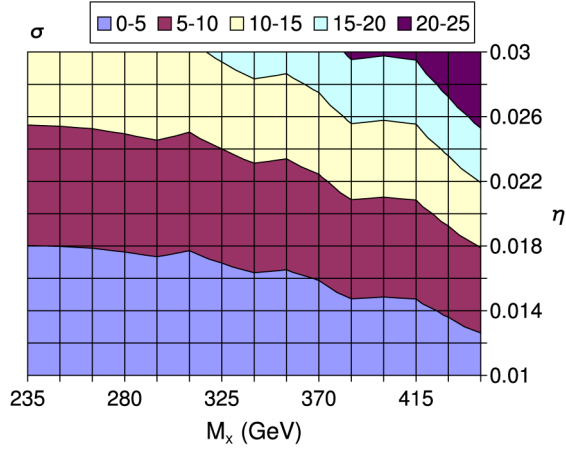
FIG. 3 (color online). Signal significance plot of $e^+e^- \rightarrow \gamma X \rightarrow \gamma \mu \bar{\mu}$ at ILC $\sqrt{s} = 500$ GeV with 500 fb^{-1} integrated luminosity. We assume that the $m_{\mu \bar{\mu}}$ can be measured to within 2%.

$$\sigma(\gamma X) = \eta^2 \frac{1.26 \times 10^{-3}}{s^2(s - m_X^2)} F(s, m_X, x_0), \quad \text{where}$$

$$F(s, m_X, x_0) = (s^2 + m_X^4)\tanh^{-1}x_0 - \frac{x_0}{2}(s - m_X^2)^2,$$

and $x_0 = |\cos\theta_{\min}| = 0.95$. Comparing this signal to the standard model background $e^+e^- \rightarrow \gamma \mu \bar{\mu}$ gives us signal significance at ILC for $m_X < 500$ GeV as well (Fig. 3). We find that kinetimatically accessible X bosons at ILC can be probed and studied perhaps better than at the LHC. Having the ILC data, along with the LHC data, can significantly help us understand all the properties of an exotic massive weakly coupled vector boson [31].

An analysis of LEP data proceeds in a similar manner. For $m_X > \sqrt{s}$, detection from LEP data is highly disfavored. For smaller m_X, however, resonance production (through hard photon emission) is allowed, which favors detection at LEP over hadron colliders such as LHC or the Tevatron. (We assume 725 pb^{-1} at $\sqrt{s} = 206$ GeV.) But
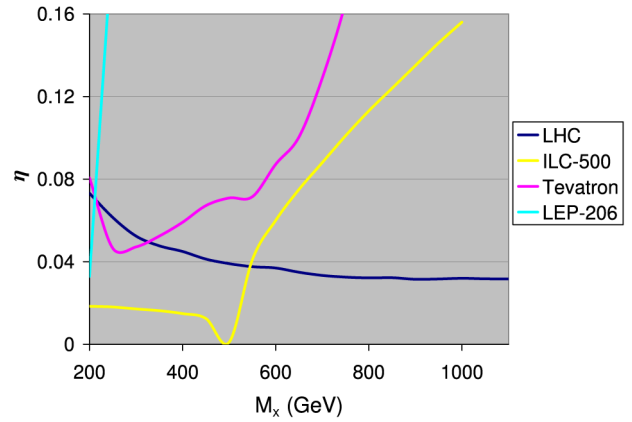

FIG. 4 (color online). Detection plot of estimated 5σ confidence level of X-boson that kinetically mixes with hypercharge. Detection for Tevatron (8 fb^{-1}), LHC (100 fb^{-1}), LEP ($\sqrt{s} = 206$ GeV, and 725 pb^{-1}), and ILC ($\sqrt{s} = 500$ GeV and 500 fb^{-1}) can occur at points above their respective lines.

even at these low m_X values ILC would provide better detection sensitivity.

VI. OUTLOOK

We can summarize our results with a detection plot (Fig. 4). We see that for $m_X \gtrsim 550$ GeV, LHC is more capable of detecting X_μ in our scenario, while for $m_X \lesssim 550$ GeV ILC-500 is more sensitive. Detection within the regime favored by a naive perturbative estimate of kinetic mixing ($\eta \sim 10^{-3} - 10^{-2}$) appears difficult at the LHC, but perhaps possible at the ILC as long as the gauge boson mass is at or below the center of mass energy of the ILC. Of course, a higher energy ILC (1 TeV and higher) will help the search for higher-mass X bosons. As we emphasized earlier, however, the amount of kinetic mixing can vary dramatically from one model to the next, depending on the multiplicity of the kinetic messengers, and thus all regions of phase space are candidates for discovery.

[1] J. L. Hewett and T. G. Rizzo, Phys. Rep. **183**, 193 (1989).
[2] M. Cvetic and P. Langacker, Phys. Rev. D **54**, 3570 (1996).
[3] A. Leike, Phys. Lett. B **402**, 374 (1997).
[4] J. Kang and P. Langacker, Phys. Rev. D **71**, 035014 (2005).
[5] J. Kumar, Int. J. Mod. Phys. A **21**, 3441 (2006).
[6] M. R. Douglas and S. Kachru, hep-th/0610102.
[7] G. Aldazabal et al., J. High Energy Phys. 02 (2001) 047.
[8] R. Blumenhagen, M. Cvetic, P. Langacker, and G. Shiu, hep-th/0502005.
[9] F. Marchesano and G. Shiu, J. High Energy Phys. 11 (2004) 041.
[10] J. Kumar and J. D. Wells, Phys. Rev. D **71**, 026009 (2005); J. High Energy Phys. 09 (2005) 067; hep-th/0604203.
[11] T. P. T. Dijkstra, L. R. Huiszoon, and A. N. Schellekens, Nucl. Phys. **B710**, 3 (2005).
[12] F. Gmeiner et al., J. High Energy Phys. 01 (2006) 004.
[13] K. R. Dienes, C. F. Kolda, and J. March-Russell, **B492**, 104 (1997).
[14] S. P. Martin, Phys. Rev. D **54**, 2340 (1996).
[15] T. G. Rizzo, Phys. Rev. D **59**, 015020 (1998).
[16] F. del Aguila, M. Masip, and M. Perez-Victoria, Nucl. Phys. **B456**, 531 (1995).
[17] B. Holdom, Phys. Lett. B **166**, 196 (1986).

[18] B. A. Dobrescu, Phys. Rev. Lett. **94**, 151802 (2005).

[19] K. S. Babu, C. F. Kolda, and J. March-Russell, Phys. Lett. B **408**, 261 (1997).

[20] S. A. Abel and B. W. Schofield, Nucl. Phys. **B685**, 150 (2004).

[21] T. Appelquist, B. A. Dobrescu, and A. R. Hopper, Phys. Rev. D **68**, 035012 (2003).

[22] M. E. Peskin and T. Takeuchi, Phys. Rev. D **46**, 381 (1992).

[23] B. Holdom, Phys. Lett. B **259**, 329 (1991).

[24] LEP Electroweak Working Group, hep-ex/0511027.

[25] W. M. Yao *et al.* (Particle Data Group), J. Phys. G **33**, 1 (2006).

[26] See, for example, ATLAS TDR, CERN Report No. CERN/LHCC/94-43, 1994 (unpublished).

[27] M. Dittmar, A. S. Nicollerat, and A. Djouadi, Phys. Lett. B **583**, 111 (2004).

[28] T. Sjostrand, S. Mrenna, and P. Skands, J. High Energy Phys. 05 (2006) 026.

[29] A. Leike, Z. Phys. C **62**, 265 (1994).

[30] A. Pukhov *et al.* (COMPHEP), hep-ph/9908288.

[31] A. Freitas, Phys. Rev. D **70**, 015008 (2004).